Detection of myocardial medium-chain fatty acid oxidation and TCA cycle activity with hyperpolarized [1-^{13}C]octanoate

(version accepted 2019-11-27)

Article DOI: 10.1002/nbm.4243

Running Title: Myocardial metabolism of hyperpolarized ^{13}C-octanoate

Hikari A.I. Yoshihara;[1,3] Jessica A.M. Bastiaansen;[3,5] Magnus Karlsson;[2,7] Mathilde H. Lerche;[2,7] Arnaud Comment;[3,6] Juerg Schwitter [1,4]

1. Division of Cardiology, Lausanne University Hospital (CHUV), Lausanne, Switzerland
2. Albeda Research ApS, Copenhagen, Denmark
3. Institute of Physics, Swiss Federal Institute of Technology (EPFL), Lausanne, Switzerland
4. Cardiac MR Center, Lausanne University Hospital (CHUV), Lausanne, Switzerland and University of Lausanne (UNIL), Lausanne, Switzerland
5. (current affiliation) Department of Diagnostic and Interventional Radiology, Lausanne University Hospital and University of Lausanne, Lausanne, Switzerland
6. (current affiliation) Cancer Research UK Cambridge Institute, University of Cambridge, Li Ka Shin Center, Robinson Way, Cambridge CB2 0RE, United Kingdom *and* General Electric Healthcare, Chalfont St Giles, Buckinghamshire HP8 4SP, United Kingdom
7. (current affiliation) Department of Health Technology, Technical University of Denmark, Kgs. Lyngby, Denmark.

Correspondence: Hikari Yoshihara

EPFL SB IPHYS LIFMET

CH-1015 Lausanne, Switzerland

hikari.yoshihara@epfl.ch

Tel: +41 21 693 6116

Word Count:

Abstract:	264
Main text:	3096
Figure legends:	189

Keywords:

beta-oxidation

dissolution DNP

hyperpolarization

cardiac

^{13}C-MRS

medium-chain triglyceride

serum albumin

Abbreviations:

FFA	free fatty acid
IBP	invasive blood pressure
PBS	phosphate buffered saline

BSA	bovine serum albumin
RPP	rate pressure product
SCAD	short-chain acyl-CoA dehydrogenase
MCAD	medium-chain acyl-CoA dehydrogenase
LCAD	long-chain acyl-CoA dehydrogenase
VLCAD	very long-chain acyl-CoA dehydrogenase
M/SCHAD	medium- short-chain L-3-hydroxyacyl-CoA dehydrogenase
MKAT	medium-chain 3-ketoacyl-CoA thiolase
TCA	tricarboxylic acid

Abstract

Under normal conditions, the heart mainly relies on fatty acid oxidation to meet its energy needs. Changes in myocardial fuel preference are noted in the diseased and failing heart. The magnetic resonance signal enhancement provided by spin hyperpolarization allows the metabolism of substrates labelled with carbon-13 to be followed in real-time in vivo. Although the low water solubility of long-chain fatty acids abrogates their hyperpolarization by dissolution dynamic nuclear polarization, medium-chain fatty acids have sufficient solubility to be efficiently polarized and dissolved. In this study we investigated applicability of hyperpolarized [1-^{13}C]octanoate to measure myocardial medium-chain fatty acid metabolism in vivo. Scanning rats infused with a bolus of hyperpolarized [1-^{13}C]octanoate, the primary metabolite observed in the heart was identified as [1-^{13}C]acetylcarnitine. Additionally, [5-^{13}C]glutamate and [5-^{13}C]citrate could be respectively resolved in 7 and 5 of 31 experiments, demonstrating the incorporation of oxidation products of octanoate into the tricarboxylic acid cycle. A variable drop in blood pressure was observed immediately following the bolus injection, and this drop correlated with a decrease in normalized acetylcarnitine signal (acetylcarnitine/octanoate). Increasing the delay before infusion moderated the decrease in blood pressure, which was attributed to the presence of residual gas bubbles in the octanoate solution. No significant difference in normalized acetylcarnitine signal was apparent between fed and 12-hour fasted rats. Compared to a solution in buffer, the longitudinal relaxation of [1-^{13}C]octanoate was accelerated approximately 3-fold in blood and by the addition of serum albumin. These results demonstrate the potential of hyperpolarized [1-^{13}C]octanoate to probe myocardial medium-chain fatty acid metabolism as well as some of the limitations that may accompany its use.

Introduction

Free fatty acids (FFAs) from stored or dietary triglycerides are the main energy source of the heart under normal conditions, with 60-90% of myocardial acetyl-CoA derived from fatty acid β-oxidation[1] and the remainder mostly provided by the oxidation of glucose- and lactate-derived pyruvate. Changes in FFA and carbohydrate utilization are noted in conditions such as heart failure[2] and ischemic heart disease, where the use of carbohydrate increases[3] and diabetes,[4] where higher levels of circulating FFAs and cardiomyocyte FFA metabolic intermediates are implicated in reduced efficiency, decreased carbohydrate utilization and insulin resistance. Changing the balance of fat vs. carbohydrate fuel utilization has been proposed as a mechanism of action of certain drugs, such as trimetazidine and ranolazine, used to treat heart failure.[5] These characteristic metabolic features of heart disease provide a strong motivation to understand better relationships between metabolic changes and myocardial disease in order to develop both improved therapies and diagnostic methods.

Although dietary fats consist mainly of long-chain triglycerides, medium-chain triglycerides are present in significant quantities in dairy products and tropical oils.[6] The catabolism of short-, medium- and long-chain fatty acids uses different ensembles of enzymes,[7] and medium-chain fatty acids are sufficiently water soluble that they do not rely on the serum protein carriers and membrane transporters used by long-chain fatty acids. Medium-chain fats are readily absorbed and preferentially catabolized rather than stored, which makes them of therapeutic interest in the treatment of obesity and metabolic syndrome.[8] The myocardial metabolism of medium-chain fatty acids has been studied by NMR spectroscopy of tissue extracts after infusion of [2,4,6,8-$^{13}C_4$]octanoate,[9,10] and the myocardium accumulated a higher amount of labeled

glutamate than the liver or a skeletal muscle, but myocardial oxidation of ketone bodies produced from octanoate in the liver[11] could account for a portion of this.

Hyperpolarized ^{13}C magnetic resonance spectroscopy (MRS) allows the metabolic fate of infused substrates labelled at privileged sites to be followed non-invasively in vivo with high sensitivity.[12] Of the available techniques, dissolution dynamic nuclear polarization (DNP) remains the most versatile and best performing method for preparing highly polarized ^{13}C-labelled substrate solutions for metabolic studies.[13] Using this technique, the myocardial metabolism of the short-chain fatty acids [1-^{13}C]acetate[14-18] and [1-^{13}C]butyrate[19-23] has been studied in rats. For acetate, the main hyperpolarized metabolites observed are acetylcarnitine and citrate, while with butyrate, metabolism to hyperpolarized glutamate, 3-hydroxybutyrate and acetoacetate is also seen. As the main physiological substrate, it would be preferable to use hyperpolarized long-chain fatty acids, but they are not amenable to the dissolution DNP process due to low water solubility. Medium-chain fatty acids are water soluble, however, but their interaction with serum albumin[24] may hasten their relaxation.[25] With this potential limitation in mind, we tested the metabolism of hyperpolarized [1-^{13}C]octanoate and report here its use and applicability as a probe of myocardial medium-chain fatty acid metabolism.

Materials and Methods

Chemicals

Deuterium oxide, [1-^{13}C]octanoic acid, sodium [1-^{13}C]acetate and [^{13}C]urea were purchased from Sigma-Aldrich (Buchs, SG, Switzerland). Octanoylcarnitine was purchased from Toronto Research Chemicals (North York, ON, Canada). [1-^{13}C]octanoic acid formulation was performed by Albeda Research (Copenhagen, Denmark).

Animals

Experiments involving animals were performed in accordance with an authorization issued by the Service de la consommation et des affaires vétérinaires (SCAV) of the Canton of Vaud, Switzerland. Male Wistar rats (n=21, 259 ± 23 g) were supplied by Charles River (Châtillon-sur-Chalaronne, France). Rats were fed a diet of normal chow, and food was removed from the cages of the fasted group the evening before the experiment (12 hr fast).

Experimental Protocol

[1-^{13}C]Octanoate polarization

40 μl of [1-^{13}C]octanoic acid (3.8 M in DMSO, 25 mM Finland trityl radical (acid form)) was added to a polytetrafluoroethylene sample cup and flash frozen with liquid nitrogen. A stoichiometric equivalent of 10 M NaOH for neutralization during dissolution was added separately to the cup. When used to reference chemical shift, [^{13}C]urea (20 μl, 5 M solution in glycerol, 26 mM OX063) was added to the sample cup separately. Experiments with sodium [1-^{13}C]acetate used a preparation (20 μl, 5 M in water, 25 mM OX063 trityl radical) that was mixed with the [^{13}C]urea solution to aid glassing and efficient polarization. Compounds were polarized with 196.80 GHz microwave irradiation in a custom-built 7 T polarizer operating at 1.0 K.[26] Upon dissolution with 6 ml of hot D_2O buffer containing 47 mM sodium phosphate, 100 mM NaCl, 2.7 mM KCl, 0.3 mM EDTA, pH 7.4, the solution of hyperpolarized compound(s) was transferred pneumatically to a phase separator/infusion pump in the scanner magnet bore,[27,28] with a delay of 5.1 s between the start of dissolution and the start of the infusion (3 s settling time). In six experiments, the delay was extended to

22.1 s to allow further settling of the solution. The [1-^{13}C]octanoate content of the infused solutions was measured by ^{1}H NMR, with [1-^{13}C]glycine (added to 33 mM) as an internal standard.

[1-^{13}C]Octanoate polarization measurement

Octanoate polarization was measured after rapid transfer to a phase separator/infusion pump equipped with ^{1}H and ^{13}C-tuned RF coils positioned in the isocenter of the 9.4 T scanner used for the in vivo experiments following the same procedure used previously.[29] Briefly, the polarized ^{13}C signal and its decay was scanned at 3 s intervals with series of 60 scans using a ~5° excitation pulse. To measure the thermal signal, gadoteric acid was added to a concentration of ~1 mM, and 256 scans were averaged using the same excitation pulse and acquisition parameters, except for a 2 s repetition time.

Animal Preparation & Monitoring

Rats were anesthetized with isoflurane (induction: 4%, surgery: 2%, scanning: 1.5 – 2%, adjusted to maintain respiration rate of ~60/min). Polyethylene catheters were installed in the femoral arteries for blood sampling and invasive blood pressure (IBP) measurements, and an additional catheter was installed in a femoral vein for infusing hyperpolarized compounds. Rats were placed supine on a holder bed and a dual-tuned ^{1}H–^{13}C surface coil (all loops with 16 mm diameter, ^{13}C in quadrature) was fixed over the heart. In two experiments to test the sensitivity to metabolites in the liver and kidney, the coil was positioned over the respective organs.

Physiology was monitored with an SA Instruments (Stony Brook, NY, USA) system using a pneumatic pillow for breathing, a rectal thermometer for body

temperature, and IBP sensor for pulse rate and blood pressure. Body temperature was maintained between 37.5 and 38.5 ºC using warm water circulating through tubing placed on the rat. Blood glucose was measured with a Reflotron Plus (Roche, Basel, Switzerland) and plasma lactate with a GM7 Micro-Stat analyzer (Analox Instruments, London, UK). At the end of seven experiments, the heart was collected and frozen for metabolite analysis by exteriorizing then excising and snap freezing it in liquid nitrogen at the moment of sacrifice.

Magnetic Resonance Imaging and Spectroscopy

MRI and MRS were performed in a 9.4 T, 31 cm horizontal bore magnet (Magnex Scientific, Oxford, UK) with a VNMRS console (Varian, Palo Alto, CA, USA). The placement of the coil was checked with gradient echo ^{1}H imaging and adjusted as needed. Shimming was performed using FAST(EST)MAP[30] with a voxel placed in the ventral side of the left ventricle and the chest above to a water line width of 35-50 Hz in ^{1}H STEAM spectra using the same voxel. A series of ^{13}C spectra was acquired, starting at the beginning of each hyperpolarized ^{13}C infusion, using BIR-4 excitation, 30º, transmitter at ~175 ppm, spectral width: 20161 Hz, acquisition time: 205 ms, WALTZ-16 ^{1}H decoupling, repetition time ~3 s with IBP pulse and respiration gating. Spectra containing [1-^{13}C]octanoate signal were summed using VnmrJ 3.2 (Agilent, Santa Clara, CA, USA) and the [1-^{13}C]octanoate and [1-^{13}C]acetylcarnitine signals were quantified by FID fitting using Bayes[31] (Washington University, St. Louis, MO, USA).

[1-^{13}C]Octanoate T_1 measurement

Sodium [1-^{13}C]octanoate dissolved in D_2O was added to phosphate buffered saline (PBS), PBS with 4.6 or 46 mg/ml bovine serum albumin (BSA), and freshly-collected whole venous blood from rats (with 200 units/ml heparin) to a final concentration of 10 mM for octanoate, 5% v/v for D_2O, and 0.46% or 4.6% w/v for BSA. The [1-^{13}C]octanoate T_1 in each of the four conditions was measured by saturation recovery to thermal polarization in three independent experiments at 310 K in a 400 MHz NMR spectrometer (AVANCE NEO, 5 mm BBFO probe, Bruker BioSpin AG Fällanden, Switzerland).

Statistics

Results are reported as mean ± standard deviation. Statistical and linear regression analyses were performed using GraphPad Prism (v. 5.04, GraphPad Software, La Jolla, CA, USA). The influence of fasting on the acetylcarnitine signal was assessed using an unpaired two-tailed Student's t-test. A p value of <0.05 was considered statistically significant.

Results

In vivo metabolism of hyperpolarized [1-^{13}C]octanoate

The signal of the hyperpolarized [1-^{13}C]octanoate bolus was detected in the heart seconds after the infusion began (Figure 1), with a chemical shift of 185.5 ppm, referenced to co-polarized [^{13}C]urea (165.48 ppm[32]). The signal intensity decreased rapidly and was no longer observable 20 to 36 s from the start of infusion. The mean injected octanoate dose was 0.17 ± 0.05 mmol/kg, and the polarization level following dissolution and transfer to the scanner bore was ~11%. Small peaks with the characteristic time-dependent signal evolution of metabolites were detected, the most

prominent of which was at 175.36 ppm, or ~10.1 ppm upfield of the octanoate peak (Figure 1a), near the reported chemical shift of [1-^{13}C]acetylcarnitine.[33] No metabolic conversion was apparent when the surface coil was placed over the liver or kidney.

To test the assignment of the metabolite, co-polarized [1-^{13}C]acetate and [^{13}C]urea were infused together, with or without polarized [1-^{13}C]octanoate. In both cases, the same metabolite peak appeared at 175.36 ppm (Figure 2), further supporting its assignment as [1-^{13}C]acetylcarnitine. An alternative assignment of [1-^{13}C]octanoylcarnitine is disfavored as in vitro ^{13}C-NMR experiments with octanoate and octanoylcarnitine show a 8.79 ppm chemical shift difference in their C-1 resonances. Other smaller metabolite peaks were observed in some experiments. [5-^{13}C]Glutamate (183.84 ppm, Figure 1) appeared on the shoulder of the [1-^{13}C]octanoate peak, and a faint broad peak at 181.1 ppm was assigned to [5-^{13}C]citrate. Compared to other hyperpolarized substrates, the [1-^{13}C]octanoate peak was notably broad in vivo with a line width at half-maximum of 96 ± 25 Hz. Although the octanoate peak often obscured the glutamate signal, the latter was clearly apparent in seven experiments (Figure S1) and citrate in five.

An immediate drop in blood pressure was noted in some hyperpolarized octanoate infusions, with a gradual recovery to pre-infusion levels. A greater drop in blood pressure upon infusion resulted in a lower relative acetylcarnitine signal (Figure 3b). A similar relationship between octanoate metabolism and the rate-pressure product (RPP) was seen (Figure S2a), but it was less apparent using the heart rate or change in heart rate (Figure S2b & c). Increasing the settling delay before the start of infusion to 20 s resulted in smaller decreases in blood pressure within the range observed using the 3 s delay (Figure 3b).

The effect of an overnight fast on the production of hyperpolarized [1-^{13}C]acetylcarnitine was also tested. Fasting significantly decreased blood glucose and lactate levels (Table 1). The acetylcarnitine signal relative to octanoate signal (acetylcarnitine/octanoate ratio) averaged 0.015 ± 0.010 in the fed rats (17 infusions) and was 0.013 ± 0.011 in fasted (14 infusions) (Figure 3a). The acetylcarnitine/octanoate ratio varied over a greater than 10-fold range in both groups and no significant difference was found. Acetylcarnitine levels measured by mass spectrometry in snap-frozen heart samples showed no significant effect of fasting (Table S1).

Longitudinal relaxation of [1-^{13}C]octanoate

In vitro ^{13}C-NMR measurements in PBS at 310 K and 9.4 T yielded a T_1 value of 32.1 ± 1.8 s for the octanoate C-1. In blood, its T_1 was shortened to 9.9 ± 1.4 s, but a value of 7.2 ± 0.8 s was measured in the presence of 4.6% BSA, indicating that interactions with serum albumin are likely responsible for the faster longitudinal relaxation in blood. The ^{13}C spectral linewidths of the octanoate carboxylate were broadened to ~20 Hz with BSA and ~68 Hz in blood (Table 2), consistent with the broad hyperpolarized octanoate peaks observed in vivo.

Discussion

We report here for the first time the myocardial metabolism of hyperpolarized [1-^{13}C]octanoate, with [1-^{13}C]acetylcarnitine the most prominent metabolite. [1-^{13}C]acetylcarnitine is similarly prominent with other hyperpolarized precursors of [1-^{13}C]acetyl-CoA, including [2-^{13}C]pyruvate,[33,34] [1-^{13}C]acetate,[16,17] [1-^{13}C]butyrate,[19,20,22] 3-hydroxy[1-^{13}C]butyrate, and [1-^{13}C]- and [3-^{13}C]acetoacetate.[23,35-38] However, each

follows a different route to acetyl-CoA. [2-^{13}C]Pyruvate conversion reflects pyruvate dehydrogenase activity, while the conversion of the ketone bodies to acetyl-CoA uses 3-oxoacid CoA-transferase and 3-ketoacyl-CoA thiolase. Conversely, acetate probes acetyl-CoA synthetase, and butyrate and octanoate respectively probe short- and medium-chain β-oxidation. Depending on the chain length, some of the steps of β-oxidation are catalyzed by different enzymes,[39] such as the acyl-CoA dehydrogenases, which are specific for short, medium, long, and very long acyl chains (SCAD, MCAD, LCAD, VLCAD, respectively). The conversion of hyperpolarized [1-^{13}C]octanoate to [1-^{13}C]acetylcarnitine indicates that the polarized state survives at least one round of β-oxidation mediated by MCAD, enoyl-CoA hydratase, medium/short-chain L-3-hydroxyacyl-CoA dehydrogenase (M/SCHAD),[40] and medium-chain 3-ketoacyl-CoA thiolase (MKAT).[41] The route of octanoate to acetylcarnitine, citrate and glutamate is summarized in Figure 4.

The low intensity of the acetylcarnitine signal relative to noise for some experiments precluded reliable kinetic analysis of the time series of spectra; however, the sum of spectra containing the octanoate signal from each infusion provided sufficient signal for relative quantitation by peak fitting. The myocardial conversion of octanoate to acetylcarnitine was not significantly different between fed and fasted rats, and while this can be at least partly attributed to the wide variability within each group, nutritional status did not significantly affect hyperpolarized butyrate to acetylcarnitine conversion.[20] However, in that study the co-infusion of hyperpolarized [1-^{13}C]butyrate and [1-^{13}C]pyruvate did increase the acetylcarnitine signal in fed rats and decreased the glutamate signal. Those results can be explained by increased flux through pyruvate dehydrogenase resulting in a larger acetylcarnitine pool[42] and more of the butyrate-derived acetyl-CoA equivalents remaining in this pool rather than entering the

tricarboxylic acid (TCA) cycle. While the bolus infusion of hyperpolarized [1-^{13}C]octanoate may also result in a transient increase in the acetylcarnitine pool, given its preferential oxidation over longer-chain fatty acids,[43] the acetylcarnitine levels in heart samples taken at the end of the experiment were not affected by fasting. Similarly, 36-48 hr fasting is reported to have negligible effects on carnitine and acetylcarnitine levels in the rat heart.[44]

During the dissolution process, the hot buffer stream melts and mixes the frozen octanoic acid preparation and frozen neutralizing sodium hydroxide solution. Because the mixing and neutralization is not instantaneous, an "acid soap" mixture of water, sodium octanoate and octanoic acid is formed early in the process. The octanoic acid molecules tend to be within mixed sodium octanoate micelles and to preferentially accumulate at air-water interfaces,[45] or form vesicles[46] which will hinder their diffusion, slowing their neutralization. The rapid dissolution and neutralization of the hyperpolarized octanoic acid results in a frothy white suspension containing small gas bubbles (Figure S3) which, while dissipating in less than one minute, imposes a delay to its infusion with the attendant polarization loss. An alternative formulation to minimize foaming during dissolution could use neutralized octanoate, such as the tris salt,[48] with the penalty of lower polarization.

The relationship between a greater drop in blood pressure upon infusion and decreased conversion to acetylcarnitine may illustrate the physiological effects of a venous air embolism. An immediate decrease in systemic blood pressure has been noted in dogs following venous injection of air,[47] similar to the decrease seen here with the infusion of the freshly-dissolved hyperpolarized octanoate mixture. Several factors could account for the decreased octanoate metabolism with lower blood pressure. These

include a reduction in myocardial perfusion as well as decreased uptake and metabolism due to the decreased cardiac workload resulting from the transient hypotension.

The physical properties of shorter chain fatty acids make them more suitable for use in dissolution-DNP. The higher water solubility of short- and medium-chain fatty acids enables their ready dissolution in aqueous solvent and their free circulation, and the slower longitudinal relaxation of quaternary carbon-13 nuclei in smaller molecules also helps extend the lifetime of the hyperpolarized state. While serum albumin dramatically enhances the solubility of long-chain fatty acids, sodium octanoate, with a critical micellar concentration of 0.39 M,[49] is readily soluble in water. It does however interact with albumin,[24] and the difference between the hyperpolarized [1-^{13}C]octanoate and [1-^{13}C]acetate signal lifetimes in vivo was notably different, with octanoate relaxing approximately twice as fast. While the accelerated longitudinal relaxation of [1-^{13}C]octanoate in blood can be explained by its interactions with albumin (Table 2), the markedly broader C-1 linewidth in blood may be due to transverse relaxation by deoxyhemoglobin or interactions with other blood components. In any case, the relatively short T_1 of [1-^{13}C]octanoate in blood is its greatest limitation as a hyperpolarized metabolic probe. For octanoate, the 1-carbon is nonetheless the best site for a hyperpolarized label. Although they were not measured in this study, the other carbons in the octanoate alkyl chain can be reasonably anticipated to have T_1 values in solution on the order of 1 – 5 s or shorter,[50] and they would be additionally decreased in blood.

Longer-chain fatty acids suffer from lower water solubility than octanoate and interact strongly with serum albumin, resulting in even faster relaxation. For example, the T_1 of [1-^{13}C]myristate, a 14-carbon fatty acid, is <1 s in a 6:1 mole ratio mix with BSA.[51] Since the physical properties limiting the performance of hyperpolarized [1-

^{13}C]octanoate as a metabolic probe are exacerbated with longer chain length, octanoate is therefore at or near the practical size limit for fatty acids using this technique.

In summary, we have demonstrated that [1-^{13}C]octanoate can be effectively hyperpolarized by dissolution DNP; however, its partly hydrophobic character greatly accelerates relaxation of the spin polarization in blood, limiting its sensitivity as a metabolic probe. Nonetheless, with its rapid metabolism in the rat heart, sufficient hyperpolarized signal survives for its uptake, β-oxidation to acetyl-CoA, and incorporation in the TCA cycle to be detected, demonstrating its potential to measure medium-chain fatty acid metabolism in vivo.

Acknowledgements

The authors thank Carola J. Romero, Corina M. Berset, Anne-Catherine Clerc, Analina da Silva, Mario Lepore and Stefan Mitrea for expert assistance with the animal experiments, the Centre d'Imagerie BioMédicale (CIBM) of the UNIL, UNIGE, HUG, CHUV, EPFL, and the Leenards and Jeantet Foundations. Quantitative mass spectral analyses of myocardial metabolite levels were performed by the Metabolomics Platform, Faculty of Biology and Medicine, University of Lausanne, Switzerland. This work was supported by Swiss National Science Foundation grants PZ00P3_167871, PP00P1_157547, 310030_138146 and 310030_163050, the Emma Muschamp foundation, and the Swiss Heart foundation.

References

1. Stanley WC, Recchia FA, Lopaschuk GD. Myocardial substrate metabolism in the normal and failing heart. *Physiol Rev*. 2005;85(3):1093-1129. doi:10.1152/physrev.00006.2004.

2. Ventura-Clapier R, Garnier A, Veksler V. Energy metabolism in heart failure. *J Physiol (Lond)*. 2004;555(Pt 1):1-13. doi:10.1113/jphysiol.2003.055095.

3. King LM, Opie LH. Glucose and glycogen utilisation in myocardial ischemia--changes in metabolism and consequences for the myocyte. *Mol Cell Biochem*. 1998;180(1-2):3-26. doi:10.1023/A:1006870419309.

4. Lopaschuk GD, Ussher JR, Folmes CDL, Jaswal JS, Stanley WC. Myocardial fatty acid metabolism in health and disease. *Physiol Rev*. 2010;90(1):207-258. doi:10.1152/physrev.00015.2009.

5. Parang P, Singh B, Arora R. Metabolic modulators for chronic cardiac ischemia. *J Cardiovasc Pharmacol Ther*. 2005;10(4):217-223.

6. Marten B, Pfeuffer M, Schrezenmeir J. Medium-chain triglycerides. *International Dairy Journal*. 2006;16(11):1374-1382. doi:10.1016/j.idairyj.2006.06.015.

7. Eaton S, Bartlett K, Pourfarzam M. Mammalian mitochondrial beta-oxidation. *Biochem J*. 1996;320 (Pt 2):345-357.

8. Nagao K, Yanagita T. Medium-chain fatty acids: functional lipids for the prevention and treatment of the metabolic syndrome. *Pharmacol Res*. 2010;61(3):208-212. doi:10.1016/j.phrs.2009.11.007.

9. Gavva SR, Wiethoff AJ, Zhao P, Malloy CR, Sherry AD. A 13C isotopomer n.m.r. method for monitoring incomplete beta-oxidation of fatty acids in intact tissue. *Biochem J*. 1994;303 (Pt 3):847-853.

10. Walton ME, Ebert D, Haller RG. Octanoate oxidation measured by 13C-NMR spectroscopy in rat skeletal muscle, heart, and liver. *J Appl Physiol*. 2003;95(5):1908-1916. doi:10.1152/japplphysiol.00909.2002.

11. McGarry JD, Foster DW. The regulation of ketogenesis from octanoic acid. The role of the tricarboxylic acid cycle and fatty acid synthesis. *J Biol Chem*. 1971;246(4):1149-1159.

12. Golman K, Zandt RIT, Thaning M. Real-time metabolic imaging. *P Natl Acad Sci Usa*. 2006;103(30):11270-11275. doi:10.1073/pnas.0601319103.

13. Comment A, Merritt ME. Hyperpolarized magnetic resonance as a sensitive detector of metabolic function. *Biochemistry*. 2014;53(47):7333-7357. doi:10.1021/bi501225t.

14. Jensen PR, Peitersen T, Karlsson M, et al. Tissue-specific short chain fatty acid metabolism and slow metabolic recovery after ischemia from hyperpolarized NMR in vivo. *J Biol Chem*. 2009;284(52):36077-36082. doi:10.1074/jbc.M109.066407.

15. Koellisch U, Gringeri CV, Rancan G, et al. Metabolic imaging of hyperpolarized [1-(13) C]acetate and [1-(13) C]acetylcarnitine - investigation of the influence of dobutamine induced stress. *Magn Reson Med*. 2014;74(4):1011-1018. doi:10.1002/mrm.25485.

16. Bastiaansen JAM, Cheng T, Lei H, Gruetter R, Comment A. Direct noninvasive estimation of myocardial tricarboxylic acid cycle flux in vivo using hyperpolarized C-13 magnetic resonance. *J Mol Cell Cardiol*. 2015;87:129-137. doi:10.1016/j.yjmcc.2015.08.012.

17. Flori A, Liserani M, Frijia F, et al. Real-time cardiac metabolism assessed with hyperpolarized [1-(13) C]acetate in a large-animal model. *Contrast Media Mol Imaging*. 2015;10(3):194-202. doi:10.1002/cmmi.1618.

18. Koellisch U, Laustsen C, Nørlinger TS, et al. Investigation of metabolic changes in STZ-induced diabetic rats with hyperpolarized [1-13C]acetate. *Physiol Rep*. 2015;3(8). doi:10.14814/phy2.12474.

19. Ball DR, Rowlands B, Dodd MS, et al. Hyperpolarized butyrate: a metabolic probe of short chain fatty acid metabolism in the heart. *Magn Reson Med*. 2014;71(5):1663-1669. doi:10.1002/mrm.24849.

20. Bastiaansen JAM, Merritt ME, Comment A. Measuring changes in substrate utilization in the myocardium in response to fasting using hyperpolarized [1-(13)C]butyrate and [1-(13)C]pyruvate. *Sci Rep*. 2016;6:25573. doi:10.1038/srep25573.

21. Bastiaansen JAM, Yoshihara HAI, Capozzi A, et al. Probing cardiac metabolism by hyperpolarized 13C MR using an exclusively endogenous substrate mixture and photo-induced nonpersistent radicals. *Magn Reson Med*. 2018;79(5):2451-2459. doi:10.1002/mrm.27122.

22. Flori A, Giovannetti G, Santarelli MF, et al. Biomolecular imaging of 13C-butyrate with dissolution-DNP: Polarization enhancement and formulation for in vivo studies. *Spectrochim Acta A*. 2018;199:153-160. doi:10.1016/j.saa.2018.03.014.

23. Abdurrachim D, Teo XQ, Woo CC, et al. Cardiac metabolic modulation upon low-carbohydrate low-protein ketogenic diet in diabetic rats studied in vivo using hyperpolarized 13 C pyruvate, butyrate, and acetoacetate probes. *Diabetes Obes Metab*. December 2018. doi:10.1111/dom.13608.

24. Kenyon MA, Hamilton JA. 13C NMR studies of the binding of medium-chain fatty acids to human serum albumin. *J Lipid Res*. 1994;35(3):458-467.

25. Lerche MH, Meier S, Jensen PR, et al. Study of molecular interactions with 13C DNP-NMR. *J Magn Reson*. 2010;203(1):52-56. doi:10.1016/j.jmr.2009.11.020.

26. Cheng T, Capozzi A, Takado Y, Balzan R, Comment A. Over 35% liquid-state (13)C polarization obtained via dissolution dynamic nuclear polarization at 7 T and 1 K using ubiquitous nitroxyl radicals. *Phys Chem Chem Phys*. 2013;15(48):20819-20822. doi:10.1039/c3cp53022a.

27. Cheng T, Mishkovsky M, Bastiaansen JAM, et al. Automated transfer and injection of hyperpolarized molecules with polarization measurement prior to in vivo NMR. *NMR Biomed*. 2013;26(11):1582-1588. doi:10.1002/nbm.2993.

28. Comment A, van den Brandt B, Uffmann K, et al. Design and performance of a DNP prepolarizer coupled to a rodent MRI scanner. *Concept Magn Reson B*. 2007;31(4):255-269.

29. Yoshihara HAI, Can E, Karlsson M, Lerche MH, Schwitter J, Comment A. High-field dissolution dynamic nuclear polarization of [1-(13)C]pyruvic acid. *Phys Chem Chem Phys*. 2016;18(18):12409-12413. doi:10.1039/c6cp00589f.

30. Gruetter R, Tkác I. Field mapping without reference scan using asymmetric echo-planar techniques. *Magn Reson Med*. 2000;43(2):319-323.

31. Marutyan KR, Bretthorst GL. The Bayesian Analysis Software Developed At Washington University. *AIP Conference Proceedings*. 2009;1193:368-381. doi:10.1063/1.3275636.

32. Wishart DS, Feunang YD, Marcu A, et al. HMDB 4.0: the human metabolome database for 2018. *Nucleic Acids Res*. 2018;46(D1):D608-D617. doi:10.1093/nar/gkx1089.

33. Schroeder MA, Atherton HJ, Ball DR, et al. Real-time assessment of Krebs cycle metabolism using hyperpolarized 13C magnetic resonance spectroscopy. *FASEB J*. 2009;23(8):2529-2538. doi:10.1096/fj.09-129171.

34. Josan S, Hurd R, Park JM, et al. Dynamic metabolic imaging of hyperpolarized [2-(13) C]pyruvate using spiral chemical shift imaging with alternating spectral band excitation. *Magn Reson Med*. 2014;71(6):2051-2058. doi:10.1002/mrm.24871.

35. Miller JJ, Ball DR, Lau AZ, Tyler DJ. Hyperpolarized ketone body metabolism in the rat heart. *NMR Biomed*. 2018;60(1):e3912. doi:10.1002/nbm.3912.

36. Abdurrachim D, Woo CC, Teo XQ, Chan WX, Radda GK, Lee PTH. A new hyperpolarized 13C ketone body probe reveals an increase in acetoacetate utilization in the diabetic rat heart. *Sci Rep*. 2019;9(1):5532. doi:10.1038/s41598-019-39378-w.

37. Abdurrachim D, Teo XQ, Woo CC, et al. Empagliflozin reduces myocardial ketone utilization while preserving glucose utilization in diabetic hypertensive heart disease: A hyperpolarized 13 C magnetic resonance spectroscopy study. *Diabetes Obes Metab*. 2018;59(1):8. doi:10.1111/dom.13536.

38. Chen W, Sharma G, Jiang W, et al. Metabolism of hyperpolarized 13 C-acetoacetate to β-hydroxybutyrate detects real-time mitochondrial redox state and dysfunction in heart tissue. *NMR Biomed*. 2019;32(6):e4091. doi:10.1002/nbm.4091.

39. Rinaldo P, Matern D, Bennett MJ. Fatty acid oxidation disorders. *Annu Rev Physiol*. 2002;64:477-502. doi:10.1146/annurev.physiol.64.082201.154705.

40. Kobayashi A, Jiang LL, Hashimoto T. Two mitochondrial 3-hydroxyacyl-CoA dehydrogenases in bovine liver. *J Biochem*. 1996;119(4):775-782.

41. Miyazawa S, Osumi T, Hashimoto T. The presence of a new 3-oxoacyl-CoA thiolase in rat liver peroxisomes. *Eur J Biochem*. 1980;103(3):589-596. doi:10.1111/j.1432-1033.1980.tb05984.x.

42. Schroeder MA, Atherton HJ, Dodd MS, et al. The cycling of acetyl-coenzyme A through acetylcarnitine buffers cardiac substrate supply: a hyperpolarized 13C magnetic resonance study. *Circ Cardiovasc Imaging*. 2012;5(2):201-209. doi:10.1161/CIRCIMAGING.111.969451.

43. Labarthe F, Gélinas R, Rosiers Des C. Medium-chain fatty acids as metabolic therapy in cardiac disease. *Cardiovasc Drugs Ther*. 2008;22(2):97-106. doi:10.1007/s10557-008-6084-0.

44. Pearson DJ, Tubbs PK. Carnitine and derivatives in rat tissues. *Biochem J*. 1967;105(3):953-963.

45. Ekwall P. Solutions of alkali soaps and water in fatty acids XI. Correlation between the acid sodium octanoate in the most water-rich part of the L2-phase and the acid soaps in two adjacent phases. *Colloid & Polymer Sci*. 1988;266(8):729-733. doi:10.1007/BF01410282.

46. Hargreaves WR, Deamer DW. Liposomes from ionic, single-chain amphiphiles. *Biochemistry*. 1978;17(18):3759-3768. doi:10.1021/bi00611a014.

47. Wycoff CC, Cann JE. Experimental pulmonary air embolism in dogs. *Calif Med*. 1966;105(5):361-367.

48. Karlsson M, Jensen PR, Duus JØ, Meier S, Lerche MH. Development of dissolution DNP-MR substrates for metabolic research. *Appl Magn Reson*. 2012;43(1-2):223-236.

49. Drakenberg T, Lindman B. 13 C NMR of micellar solutions. *Journal of Colloid and Interface Science*. 1973;44(1):184-186.

50. Allerhand A, Doddrell D. Segmental motion in liquid 1-decanol. Application of natural-abundance carbon-13 partially relaxed Fourier transform nuclear magnetic resonance. J Am Chem Soc. 1971;93(6):1558-1559. doi:10.1021/ja00735a072.

51. Hamilton JA, Cistola DP, Morrisett JD, Sparrow JT, Small DM. Interactions of myristic acid with bovine serum albumin: a 13C NMR study. *P Natl Acad Sci Usa*. 1984;81(12):3718-3722.

Figure legends

Figure 1. A) Representative time course of hyperpolarized [1-^{13}C]octanoate metabolism in the rat heart, showing the evolution of the [1-^{13}C]acetylcarnitine and [5-^{13}C]glutamate signals and the rapid relaxation of the octanoate. B) Sum of metabolite-containing spectra from a single infusion showing conversion of octanoate to glutamate, citrate and acetylcarnitine.

Figure 2. Identification of the main octanoate metabolite. Overlay of experiments infusing hyperpolarized [1-^{13}C]octanoate (bottom trace, thick line), [1-^{13}C]acetate (middle trace, medium line), and a mixture of both (top trace, thin line) all show [1-^{13}C]acetylcarnitine (175.36 ppm) as the primary metabolite. Spectra were referenced to co-polarized [^{13}C]urea (165.48 ppm, not pictured).

Figure 3. A) Myocardial [1-^{13}C]acetylcarnitine / [1-^{13}C]octanoate signal ratio in fed and fasted rats. B) Relationship between blood pressure (BP) drop upon infusion and decreased acetylcarnitine/octanoate ratio. Change in systolic (Sys) BP 15 s from start of infusion, plotted in the x-axis, corresponds approximately to the time of peak metabolite signal. Squares indicate experiments where infusion was delayed 20 s (as opposed to 3 s) to allow further liquid settling prior to infusion.

Figure 4. Summary of metabolic pathways engaged by hyperpolarized [1-^{13}C]octanoate, highlighting the paths to the metabolites detected.

Tables

Table 1. Arterial blood glucose and lactate levels in fed and fasted rats

	Fed	Fasted
# of measurements	13	17
Blood glucose (mg/dl)	131 ± 29	91 ± 24
Blood lactic acid (mg/dl)	17.3 ± 4.9	9.0 ± 4.8

Table 2. In vitro longitudinal relaxation of [1-^{13}C]octanoate at 9.4 T & 37ºC

Solvent	T_1 (s)	Linewidth (Hz)
PBS	32.1 ± 1.8	0.9 ± 0.2
PBS + 0.46% (w/v) BSA	23.0 ± 1.7	5.7 ± 0.1
PBS + 4.6% (w/v) BSA	7.2 ± 0.8	20 ± 1
venous rat blood w/ heparin	9.9 ± 1.4	68 ± 13

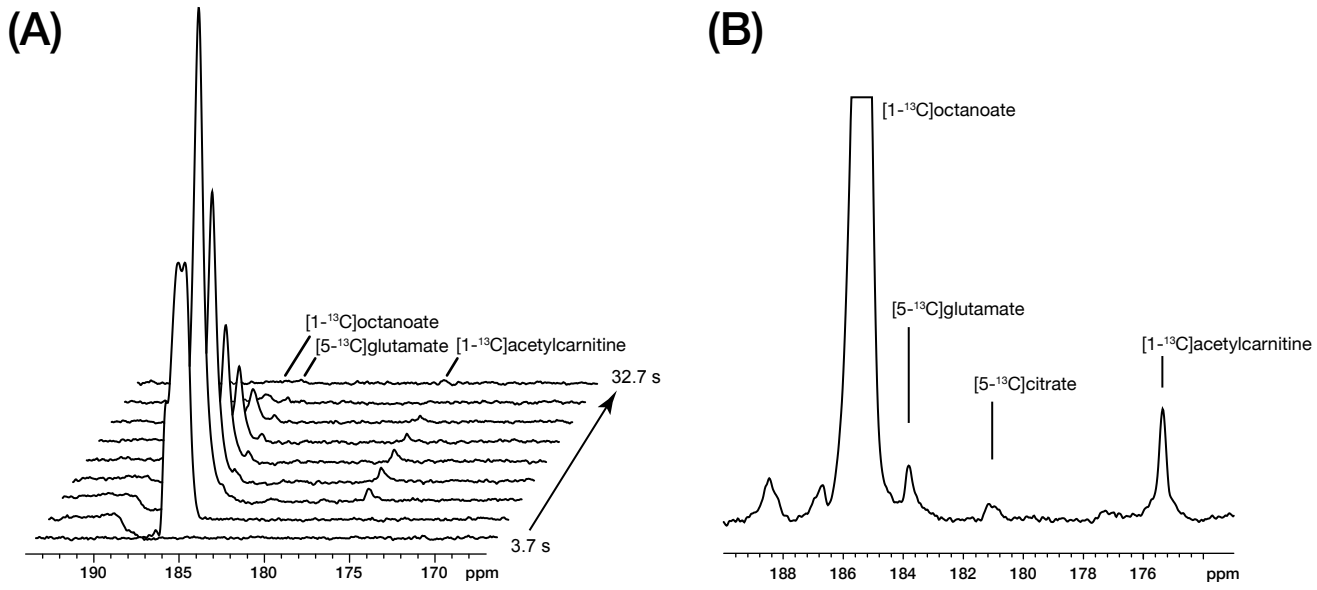
(A)
[1-13C]octanoate
[5-13C]glutamate
[1-13C]acetylcarnitine
32.7 s
3.7 s
190
185
180
175
170
ppm
(B)
[1-13C]octanoate
[5-13C]glutamate
[5-13C]citrate
[1-13C]acetylcarnitine
188
186
184
182
180
178
176
ppm

Figure 1

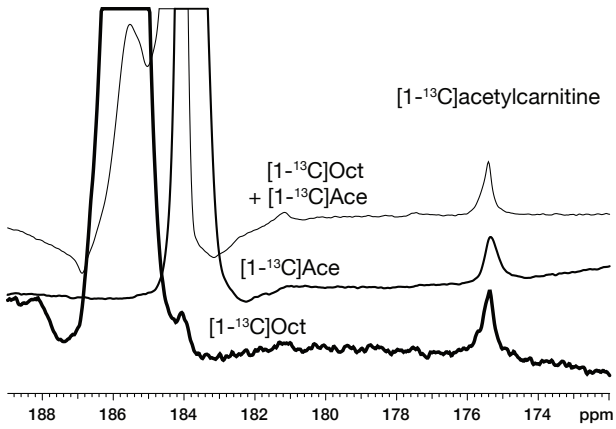
[1-13C]acetylcarnitine
[1-13C]Oct
+ [1-13C]Ace
[1-13C]Ace
[1-13C]Oct
188
186
184
182
180
178
176
174
ppm

Figure 2

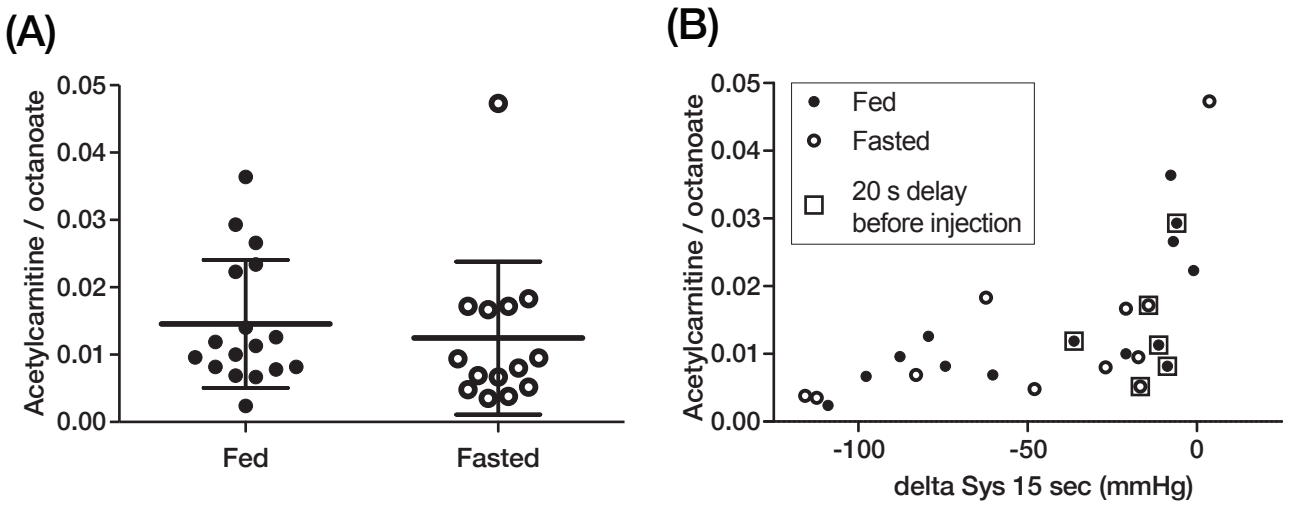
(A)
Acetylcarnitine / octanoate
0.05
0.04
0.03
0.02
0.01
0.00
Fed
Fasted
(B)
Acetylcarnitine / octanoate
0.05
0.04
0.03
0.02
0.01
0.00
Fed
Fasted
20 s delay
before injection
-100
-50
0
delta Sys 15 sec (mmHg)

Figure 3

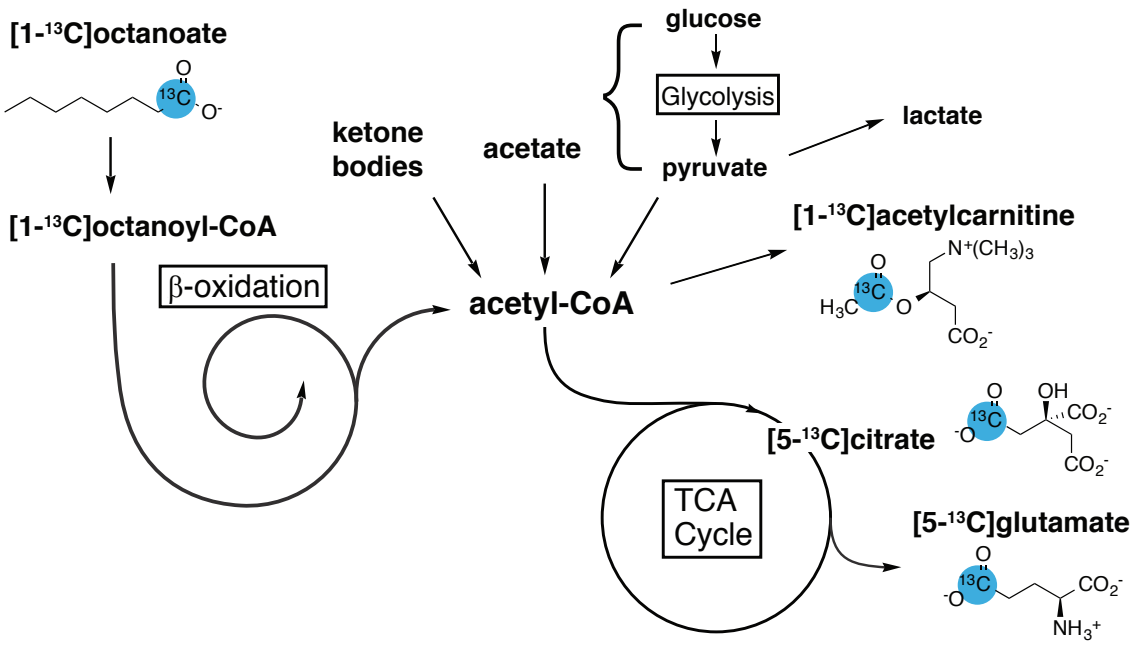
[1-13C]octanoate
[1-13C]octanoyl-CoA
β-oxidation
ketone bodies
acetate
glucose
Glycolysis
pyruvate
lactate
acetyl-CoA
[1-13C]acetylcarnitine
[5-13C]citrate
TCA Cycle
[5-13C]glutamate

Figure 4